Special Issue on Chemistry

Neem Leaf Extract Assisted Biosynthesis and Characterization Studies of Spinel $NiFe_2O_4$ Nanoparticles

K. Mullai, B. Muthu and A. Manikandan

Issue Editor
Dr. A. Manikandan

Research Journal of Agricultural Sciences
An International Journal

P- ISSN: 0976-1675
E- ISSN: 2249-4538

Volume: 13
Issue: Special

Res. Jr. of Agril. Sci. (2022) 13(S): 079–082

CARAS

Res. Jr. of Agril. Sci. (2022) 13(Special): 079–082

www.rjas.org

ISSN: 0976-1675 (P)
ISSN: 2249-4538 (E)

Full Length Research Article

Neem Leaf Extract Assisted Biosynthesis and Characterization Studies of Spinel $NiFe_2O_4$ Nanoparticles

K. Mullai[1], B. Muthu[2] and A. Manikandan*[3]

Received: 07 Dec 2021 | Revised accepted: 15 Feb 2022 | Published online: 25 Feb 2022

ABSTRACT

In this study, nickel ferrite ($NiFe_2O_4$) magnetic nanoparticles (NPs) were synthesized using *Neem leaf* (*Azadirachta indica*) extract and nickel nitrate as precursors. Physical and chemical properties of $NiFe_2O_4$ NPs were determined by scanning electron microscopy (FE-SEM), transmission electron microscopy (TEM), X-ray diffraction (XRD), vibrating sample magnetometry (VSM), and energy dispersive X-ray (EDS) analysis. The photocatalytic dye degradation effect of $NiFe_2O_4$ NPs against methylene blue (MB) was evaluated based photocatalytic reactor. SEM results demonstrated ceramic spinel $NiFe_2O_4$ NPs with spherical surface morphologies. It appears that these $NiFe_2O_4$ NPs can be considered as suitable candidates for photocatalyst for the dye degradation and other biomedical applications, because of their higher catalytic active effects.

***Key words*:** $NiFe_2O_4$ NPs, Neem leaf extract, Bio-synthesis, Magnetic properties, Photocatalysts

Recently, nickel ferrites ($NiFe_2O_4$) NPs are ceramic nanoscale materials [1], which can be deployed different applications. Recent findings suggest that a number of nanomaterials induce dye degradation effects [1]. These nanomaterials are deployed due to their nanometer size, catalytic properties [2], surface plasmonic resonance [3], magnetic properties [4], etc. In recent decades, ferrite magnetic NPs with the chemical formula of MFe_2O_4 (M = Ni, Co, Cu, etc.) [5] have attracted the attention of researchers in various biomedical fields including photocatalyst [6], hyperthermia [7], labelling of cells [8], etc. Spinel ferrite NPs can be employed as magnetic resonance imaging (MRI) contrast agents [9-10]. In this study, $NiFe_2O_4$ NPs were eco-friendly synthesized using *Neem leaf* (*Azadirachta indica*) extract. The physical and chemical properties of the $NiFe_2O_4$ NPs were determined by powder X-ray diffraction (XRD), scanning electron microscopy (SEM), transmission electron microscopy (TEM), and vibrating-sample magnetometer (VSM) analyses. Finally, the photocatalytic degradation effect of them was evaluated against methylene blue (MB).

MATERIALS AND METHODS

Iron (III) nitrate, nickel (II) nitrate (Sigma-Aldrich, 99%), and *Neem leaf* (*Azadirachta indica*) extract were utilized for the green synthesis of $NiFe_2O_4$ NPs. Deionized water was utilized in all stages of the synthesis. Methylene blue (MB) was purchased for the photocatalytic degradation. The *Neem leaf* (*Azadirachta indica*) extract were washed with deionized water. Plant moisture was removed at 50 °C. To each gram of watercress powder, 10 ml of deionized water was added and shaken at 50°C, overnight. Finally, the extract was separated with Whatman paper and centrifuged. Iron (III) nitrate, nickel (II) nitrate solution was added to 50 ml of aqueous extract. The mixture was kept in a microwave oven. The final product were washed well with DI water and ethanol twice finally dried at 70°C and used for further characterizations.

Characterization techniques

The structural characterization of $NiFe_2O_4$ NPs were performed using Rigaku Ultima X-ray diffractometer equipped with Cu-Kα radiation (λ =1.5418 Å). The surface functional groups were analyzed by Perkin Elmer FT-IR spectrometer. Morphological studies and energy dispersive X-ray analysis (EDX) of $NiFe_2O_4$ NPs have been performed with a Jeol JSM6360 high resolution scanning electron microscopy (HR-SEM). UV-Visible diffuse reflectance spectrum (DRS) was recorded using Cary100 UV-Visible spectrophotometer to estimate their band gap energy (E_g). Magnetic measurements were carried out at room temperature using a PMC MicroMag 3900 model vibrating sample magnetometer equipped with 1 Tesla magnet.

RESULTS AND DISCUSSION

Powder XRD analysis

* **A. Manikandan**
✉ manikandana.che@bharathuniv.ac.in

[1-3] Department of Chemistry, Bharath Institute of Higher Education and Research (BIHER), Chennai - 600 073, Tamil Nadu, India

Fig 1 shows the XRD diagram of $NiFe_2O_4$ NPs shows 5 sharp peaks at 2θ= 30°, 35.9°, 43°, 57.2°, and 62.8°. The peaks mentioned in two XRD spectra correspond to the cubic spinel structure of the $NiFe_2O_4$ NPs [11-13]. The crystallization degree of $NiFe_2O_4$ NPs depends on the synthesis procedure, temperature and time. The average crystallite size of $NiFe_2O_4$ NPs was calculated using Debye Scherrer formula given in eqn. 1:

$$L = \frac{0.89\lambda}{\beta\cos\theta} \quad \text{--- (1)}$$

where L is the crystallite size, λ, the X-ray wavelength, θ, the Bragg diffraction angle and β, the full width at half maximum (FWHM). The average crystallite size 'L' calculated from the diffraction peaks was found to be around 15 nm.

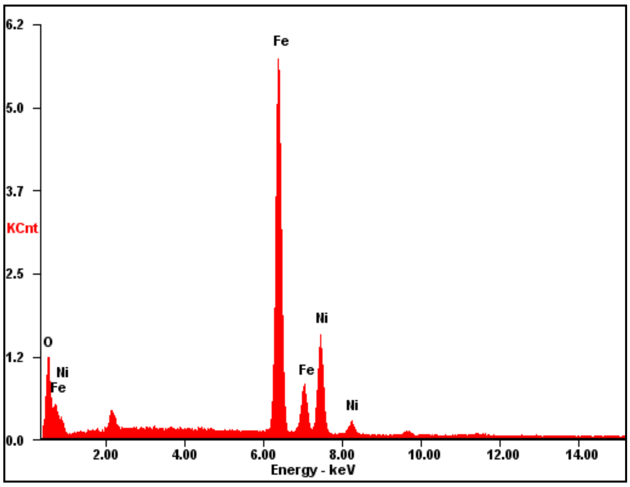

Fig 1 Powder XRD diagram of $NiFe_2O_4$ NPs

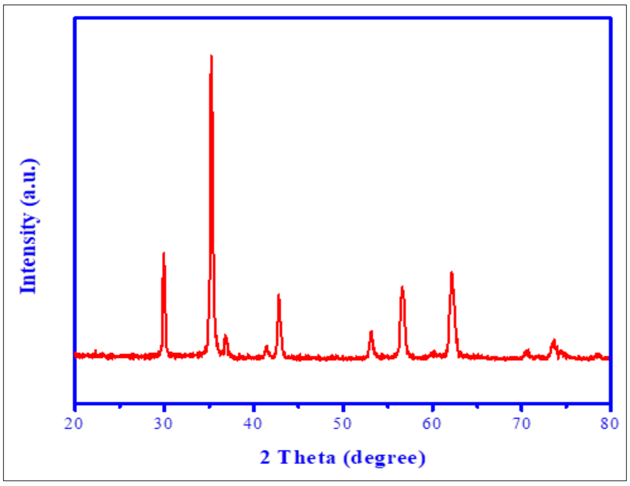

Fig 2 HR-SEM image of $NiFe_2O_4$ NPs

SEM studies

Figure 2 shows HR-SEM images of the prepared $NiFe_2O_4$ NPs. The comparison of SEM images and XRD spectra shows the difference in crystallization of $NiFe_2O_4$ NPs. SEM images of the $NiFe_2O_4$ NPs confirmed the spherical surface morphology. Cubic and sheet-shaped plates with 16 to 14 nm wide illustrated that the NPs are crystallized well in a short time by the microwave heating. As the crystallization time increases, the particles are formed in a regular and spherical way of 15 to 20 nm. Based on the results, by increasing the crystallization time, $NiFe_2O_4$ NPs were more spherical and smaller with higher purity [14-15].

EDX studies

The presence of the element Ni, Fe and O confirmed the pure phase formation. However, the presence of carbon element in the EDX diagram was due to the residues of the *Neem leaf* (*Azadirachta indica*) extract in the structure of $NiFe_2O_4$ NPs (Fig 3).

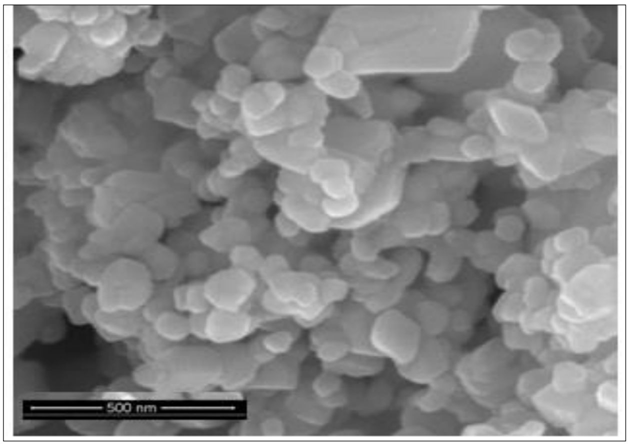

Fig 3 EDX diagram of $NiFe_2O_4$ NPs

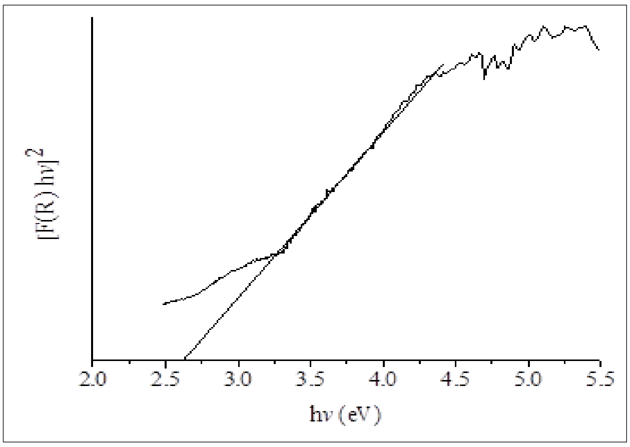

Fig 4 Band gap energy (E_g) of $NiFe_2O_4$ NPs

Optical properties

The band gap energy (E_g) of $NiFe_2O_4$ NPs can be evaluated using the Kubelka - Munk model. UV-Vis. diffuse reflectance (UV-DRS) spectra of $NiFe_2O_4$ NPs were shown in Figure 4 and the band gap energy E_g 2.58, indicating that $NiFe_2O_4$ NPs exhibited an intense absorption in the visible range [16-18]. DRS analysis was used to study the relation of crystallite size and band gap of the semiconductors. Kubelka-Munk function, *F(R)* is directly proportional to the absorption coefficient (α) and the value is estimated from the following eqn. 2,

$$(F(R)) = \alpha = \frac{(1-R)^2}{2R} \quad \text{---- (2)}$$

where, *F(R)* is Kubelka-Munk function, α, the absorbance, *R*, the reflectance. A graph is plotted between $[F(R)h\upsilon]^2$ and hυ, the obtained intercept value is the E_g of the $NiFe_2O_4$ NPs. The estimated E_g of $NiFe_2O_4$ NPs is 2.58 eV.

Magnetic properties

The magnetic properties of $NiFe_2O_4$ NPs at room temperature (RT) and ±15kOe applied field are shown in (Fig 5). The amount of magnetic saturation (M_s) for the synthesized

$NiFe_2O_4$ NPs was 62.54emu/g. The obtained result shows superparamagnetic properties [19-21]. Additionally, the amount of magnetic saturation of $NiFe_2O_4$ NPs depends on their size, crystallinity and structure [22-25]. The spinel structure and superparamagnetic behaviour of $NiFe_2O_4$ NPs were confirmed by XRD and VSM analyses.

Photocatalytic properties

The photocatalytic dye degradation effect was evaluated against methylene blue (MB) dye using UV-Visible irradiation and observed enhanced PCD efficiency [26-28]. According to the literature, $NiFe_2O_4$ NPs are the best catalytic agents for the organic dye degradation. Nickel ions increased the surface to volume ratio in $NiFe_2O_4$ NPs, thus demonstrating good photocatalytic properties against organic dyes, methylene blue (MB) [29-31].

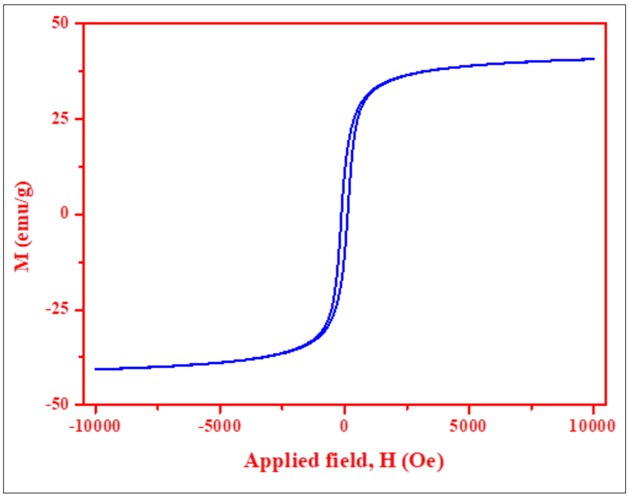

Fig 5 Magnetic properties of $NiFe_2O_4$ NPs

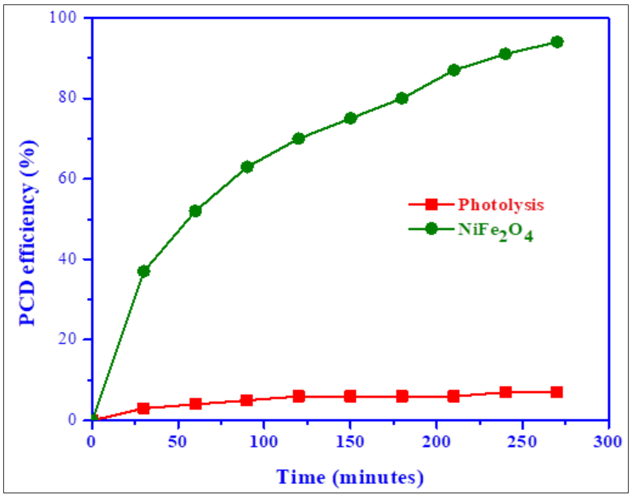

Fig 6 PCD efficiency of $NiFe_2O_4$ NPs.

CONCLUSION

In this study, $NiFe_2O_4$ NPs were synthesized using aqueous extract of *Neem leaf* (*Azadirachta indica*) via a simple and green method. Physical and chemical properties of $NiFe_2O_4$ NPs were evaluated by powder XRD, HR-SEM, EDX and VSM analyses. The photocatalytic dye degradation effect was evaluated against methylene blue (MB) dye using UV-Visible irradiation and observed enhanced PCD efficiency.

Acknowledgment

The authors are thankful to Tamil Nadu State Council for Science and Technology (TNSCST), DOTE Campus, Chennai for the financial support (S&T Project: TNSCST/ STP-PRG/AR/2018-2019/9307).

LITERATURE CITED

1. A. Manikandan, R. Sridhar, S. A. Antony, S. Ramakrishna, A simple aloe vera plant-extracted microwave and conventional combustion synthesis: Morphological, optical and catalytic properties of magnetic $CoFe_2O_4$ nanostructures, J. Mol. Struct., 1076 (2014) 188-200.
2. N. Babitha, L. Srimathi Priya, S. Rosy Christy, A. Manikandan, A. Dinesh, M. Durka, and S. Arunadevi, Enhanced Antibacterial Activity and Photo-Catalytic Properties of ZnO Nanoparticles: Pedalium Murex Plant Extract-Assisted Synthesis, J. Nanoscie. Nanotech. 19 (2019) 2888–2894.
3. K. Chitra, A. Manikandan, S. Arul Antony, Effect of poloxamer on Zingiber officinale extracted green synthesis and antibacterial studies of silver nanoparticles, J. Nanoscie. Nanotech. 16 (2016) 758-764.
4. A. Manikandan, M. Durka, S. Arul Antony, Hibiscus rosa-sinensis leaf extracted green methods, magneto-optical and catalytic properties of spinel $CuFe_2O_4$ nano- and microstructures, J. Inorg. Organomet. Polym., 25 (2015) 1019–1031.
5. K. Chitra, K. Reena, A. Manikandan, S. Arul Antony, Antibacterial studies and effect of poloxamer on gold nanoparticles by Zingiber officinale extracted green synthesis, J. Nanoscie. Nanotech. 15 (2015) 4984-4991.
6. K. Chitra, A. Manikandan, S. Moortheswaran, K. Reena, S. Arul Antony, Zingiber officinale extracted green synthesis of copper nanoparticles: Structural, morphological and antibacterial studies, Adv. Sci. Eng. Med., 7 (2015) 710-716.
7. A. Manikandan, M. Durka, M. A. Selvi, S. Arul Antony, Sesamum indicum plant extracted microwave combustion synthesis and opto-magnetic properties of spinel $Mn_xCo_{1-x}Al_2O_4$ nano-catalysts, J. Nanoscie. Nanotech. 16 (2016) 448-456.
8. A. Manikandan, M. Durka, M. A. Selvi, S. Arul Antony, Aloe vera plant extracted green synthesis, structural and opto-magnetic characterizations of spinel $Co_xZn_{1-x}Al_2O_4$ nano-catalysts, J. Nanoscie. Nanotech. 16 (2016) 357-373.
9. P. Bhavani, A. Manikandan, P. Paulraj, A. Dinesh, M. Durka, and S. Arul Antony, Okra (Abelmoschus esculentus) Plant Extract-Assisted Combustion Synthesis and Characterization Studies of Spinel $ZnAl_2O_4$ Nano-Catalysts, J. Nanoscie. Nanotech. 18 (2018) 4072–4081.
10. D. Maruthamani, S. Vadivel, M. Kumaravel, B. Saravanakumar, B. Paul, S. Sankar Dhar, A. H. Yangjeh, A. Manikandan, G. Ramadoss, Facile synthesis of Bi_2O_3/reduced graphene oxide (RGO) nanocomposite for supercapacitor and visible light photocatalytic applications, J. Colloid Interf. Sci., 498 (2017) 449-459.
11. A. Shameem, P. Devendran, V. Siva, M. Raja, A. Manikandan, S. A. Bahadur, Preparation and characterization studies of nanostructured CdO thin films by SILAR method for photocatalytic applications, J. Inorg. Organomet. Polym., 27 (2017) 692–699.

12. A. Silambarasu, A. Manikandan, K. Balakrishnan, Room temperature superparamagnetism and enhanced photocatalytic activity of magnetically reusable spinel $ZnFe_2O_4$ nano-catalysts, J. Supercond. Nov. Magn., 30 (2017) 2631–2640.
13. R. Bomila, S. Srinivasan, S. Gunasekaran, A. Manikandan, Enhanced photocatalytic degradation of methylene blue dye, opto-magnetic and antibacterial behaviour of pure and La-doped ZnO nanoparticles, J. Supercond. Nov. Magn., 31 (2018) 855–864.
14. I. J. C. Lynda, M. Durka, A. Dinesh, A. Manikandan, S. K. Jaganathan, A. Baykal, S. Arul Antony, Enhanced Magneto-optical and Photocatalytic Properties of Ferromagnetic $Mg_{1-y}Ni_yFe_2O_4$ ($0.0 \leq y \leq 1.0$) Spinel Nano-ferrites, J. Supercond. Nov. Magn., 31 (2018) 3637–3647.
15. S. Velanganni, A. Manikandan, J. Joseph Prince, C. Neela Mohan, R. Thiruneelakandan, Nanostructured ZnO coated Bi_2S_3 thin films: Enhanced photocatalytic degradation of Methylene blue dye, Physica B, 545 (2018) 383-389.
16. J. A. H. Sheela, S. Lakshmanan, A. Manikandan, S. A. Antony, Structural, morphological and optical properties of ZnO, ZnO:Ni^{2+} and ZnO:Co^{2+} nanostructures by hydrothermal process and their photocatalytic activity, J. Inorg. Organomet. Polym. 28 (2018) 2388–2398.
17. R. A. Senthil, S. Osman, J. Pan, Y. Sun, T. R. Kumar, A. Manikandan, A facile hydrothermal synthesis of visible-light responsive $BiFeWO_6/MoS_2$ composite as superior photocatalyst for degradation of organic pollutants, Ceram. Int., 45 (2019) 18683-18690.
18. R. A. Senthil, S. Osman, J. Pan, A. Khan, V. Yang, T. R. Kumar, Y. Sun, A. Manikandan, One-pot preparation of AgBr/α-Ag_2WO_4 composites with superior photocatalytic activity under visible-light irradiation, Colloids and Surf. A: Physicochem. Eng. Aspects, 586 (2020) 124079.
19. S. Rathinavel, R. Deepika, D. Panda, A. Manikandan, Synthesis and characterization of $MgFe_2O_4$ and $MgFe_2O_4$/rGO nanocomposites for the photocatalytic degradation of methylene blue, Inorg. Nano-Metal Chem., 51, 2 (2021) 210-217.
20. A Muthukrishnaraj, SS Kalaivani, A Manikandan, Helen P Kavitha, R Srinivasan, N Balasubramanian, Sonochemical synthesis and visible light induced photocatalytic property of reduced graphene oxide@ ZnO hexagonal hollow rod nanocomposite, J. Alloys Compds., 83625 (2020) 155377.
21. T. L. Ajeesha, A. Ashwini, Mary George, A. Manikandan, J. Arul Mary, Y. Slimani, M. A. Almessiere, A. Baykal, Nickel substituted $MgFe_2O_4$ nanoparticles via co-precipitation method for photocatalytic applications, Physica B, 606 (2021) 412660.
22. R. Renuga, A. Manikandan, J. A. Mary, A. Muthukrishnaraj, A. Khan, S. Srinivasan, B. Abdullah M. Al Alwan and K. M. Khedher, Enhanced Magneto-Optical, Morphological, and Photocatalytic Properties of Nickel-Substituted SnO_2 Nanoparticles, J. Supercond. Nov. Magn., 34 (2021) 825–836.
23. M. George, T.L. Ajeesha, A. Manikandan, Ashwini Anantharaman, R.S. Jansi, E. Ranjith Kumar, Y. Slimani, M.A. Almessiere, A. Baykal, Evaluation of Cu-$MgFe_2O_4$ spinel nanoparticles for photocatalytic and antimicrobial activates. J. Phys. Chem. Solids, 153 (2021) 110010.
24. K. Geetha, R. Udhayakumar, A. Manikandan, Enhanced magnetic and photocatalytic characteristics of cerium substituted spinel $MgFe_2O_4$ ferrite nanoparticles, Physica B, 615 (2021) 413083.
25. C. Sambathkumar, V. Manirathinam, A. Manikandan, M. Krishna Kumar, S. Sudhakar, P. Devendran, Solvothermal synthesis of Bi_2S_3 nanoparticles for active photocatalytic and energy storage device applications, J. Mater. Sci. Mater. Elect., 32 (2021) 20827-20843.
26. SP Ratnayake, M Mantilaka, C Sandaruwan, D Dahanayake, E Murugan, Carbon quantum dots-decorated nano-zirconia: a highly efficient photocatalyst, Applied Catalysis A: General, 2019, 570, 23-30.
27. E Murugan, I Pakrudheen, Efficient amphiphilic poly (propylene imine) dendrimer encapsulated ruthenium nanoparticles for sensing and catalysis applications, Science of Advanced Materials, 2015, 7 (5), 891-901.
28. E Murugan, JN Jebaranjitham, A Usha Synthesis of polymer-supported dendritic palladium nanoparticle catalysts for Suzuki coupling reaction, Applied Nanoscience, 2012, 2 (3), 211-222
29. E Murugan, SS Kumar, KM Reshna, S Govindaraju, Highly sensitive, stable g-CN decorated with AgNPs for SERS sensing of toluidine blue and catalytic reduction of crystal violet, Journal of Materials Science 2019, 54 (7), 5294-5310
30. E Murugan, S Santhoshkumar, S Govindaraju, M Palanichamy, Silver nanoparticles decorated g-C3N4: An efficient SERS substrate for monitoring catalytic reduction and selective Hg2+ ions detection, Spectrochimica Acta Part A: Molecular and Biomolecular Spectroscopy, 2021, 246, 119036.
31. E Murugan, R Rangasamy, Development of stable pollution free TiO2/Au nanoparticle immobilized green photo catalyst for degradation of methyl orange, Journal of Biomedical Nanotechnology, 2011, 7 (1), 225-228.